Original research article

IJAO The International Journal of Artificial Organs

Ultrasonic mixing chamber as an effective tool for the biofabrication of fully graded scaffolds for interface tissue engineering

The International Journal of Artificial Organs
2019, Vol. 42(10) 586–594

DOI: 10.1177/0391398819852960
journals.sagepub.com/home/jao
SAGE

Irene Chiesa[1], Gabriele Maria Fortunato[1,2], Anna Lapomarda[1,2], Licia Di Pietro[1,2], Francesco Biagini[1,2], Aurora De Acutis[1,2], Luca Bernazzani[3], Maria Rosaria Tinè[3], Carmelo De Maria[1,2] and Giovanni Vozzi[1,2]

Abstract

One of the main challenges of the interface-tissue engineering is the regeneration of diseased or damaged interfacial native tissues that are heterogeneous both in composition and in structure. In order to achieve this objective, innovative fabrication techniques have to be investigated. This work describes the design, fabrication, and validation of a novel mixing system to be integrated into a double-extruder bioprinter, based on an ultrasonic probe included into a mixing chamber. To validate the quality and the influence of mixing time, different nanohydroxyapatite–gelatin samples were printed. Mechanical characterization, micro-computed tomography, and thermogravimetric analysis were carried out. Samples obtained from three-dimensional bioprinting using the mixing chamber were compared to samples obtained by deposition of the same final solution obtained by manually operated ultrasound probe, showing no statistical differences. Results obtained from samples characterization allow to consider the proposed mixing system as a promising tool for the fabrication of graduated structures which are increasingly being used in interface-tissue engineering.

Keywords

Interface-tissue engineering, multi-extruder bioprinter, biofabrication, ultrasonic probe, graded scaffold

Date received: 6 February 2019; accepted: 6 May 2019

Introduction

Interface-tissue engineering (ITE) is a growing research field driven by the goal to fabricate biological substitutes aiming to repair or regenerate the functions of diseased or damaged interfacial native tissues, which exist as transitional and heterogeneous zones between different tissues.[1] The "soft-to-hard" tissue interfaces play a crucial role for joint motion and stabilization, whose regeneration can provide a successful treatment to people suffering of musculoskeletal injuries, such as damage to soft tissue-to-bone connections[2,3] or cartilage-to-bone transition.[1,4]

Current approach in ITE is represented by the scaffold-based strategy.[5,6] A well-designed tissue-engineered scaffold should mimic the extracellular matrix (ECM) of the host tissue from the mechanical, topological, physical, and biochemical point of view.[7] When designing a scaffold, the selection of the scaffolding-biomaterials and the inclusion of biochemical and biophysical stimuli are crucial points.[5] In addition, providing an ECM-like highly controlled micro- and nano-architecture plays a significant role to guarantee an adequate nutrient and waste transport, mechanical stability, and cellular interactions.[8]

[1]Research Center "E. Piaggio," University of Pisa, Pisa, Italy
[2]Department of Ingegneria dell'Informazione, University of Pisa, Pisa, Italy
[3]Department of Chemistry and Industrial Chemistry, University of Pisa, Pisa, Italy

Corresponding author:
Giovanni Vozzi, Department of Ingegneria dell'Informazione, University of Pisa, Largo Lucio Lazzarino, 1, 56122 Pisa, Italy.
Email: g.vozzi@ing.unipi.it

Nevertheless, interface tissues consist of heterogeneous distributions of cell types and ECM components with gradients of architecture and properties.[9] Therefore, the conventional scaffolding approach has a crucial limitation in ITE due to the use of biomaterials with homogenously distributed composition and properties.[1,10]

Thus, it is unsurprising that new materials, design, and fabrication approaches are needed to overcome the lack of heterogeneity within conventional scaffolds improving their biomimicry for ITE purposes.

The advent of additive manufacturing (AM) technologies within the TE field (*bioprinting*)[11,12] has made possible the fabrication of ITE structures with a complex and graded topological organization that mimics the native tissue architecture, irreproducible with the traditional strategies.[9,13] Different AM approaches are used for topological gradient objectives.[14–16] Nevertheless, bioprinting for ITE is still facing several technical and theoretical challenges for the development of scaffolds with controllable anisotropy, heterogeneity, and gradients in compositional and functional properties both at the macro and micro scales.[1,17]

Extrusion-based bioprinters have been considered the most promising approach for achieving a clinically relevant construct,[18] thanks to multi-extruders system, which can be sequentially selected, or to multi-reservoirs, which will feed a single nozzle.[17]

In the latter case, the use of microfluidic system was reported for modulating scaffold composition;[19,20] however, these systems can encounter blocking problems and are usually well suited only for low-viscosity solutions.[21]

To overcome these limitations and fabricate scaffolds that better recapitulate soft-to-bone tissue interfaces, this work presents the design and fabrication of a novel ultrasonic mixing chamber capable of mixing two materials into a homogeneous dispersion immediately before its deposition. The presented system was integrated into a double-nozzle piston-driven extruder of a home-made bioprinter to fabricate fully graded scaffolds (FGS) through a precise control deposition.

On the basis of our previous works, genipin–crosslinked gelatin solution and nanohydroxyapatite–gelatin solution were chosen, respectively, as soft and hard materials to be mixed by the presented chamber.[22–26]

Preliminary tests were carried out to validate the effectiveness of the mixing chamber for ITE applications, and finally, a bioprinting test was performed to assess the capability of fabricating structures enriched with a composition gradient.

Materials and methods

Mixing tool design and fabrication

A mixing chamber for a double-extruder three-dimensional (3D)-bioprinter was designed and fabricated to achieve the direct fabrication of FGS, considering the need of mixing composite materials into homogeneous dispersions with a controlled and tunable composition over time, by using ultrasounds produced by a probe-sonicator.

The material of the chamber had to be adequately compliant and though in order to absorb ultrasounds energy without breaking and degrading during the printing processes. A single-piece chamber without sharp edges was required to avoid both the leakage of the material during its use and the accumulation of unmixed material in the edges which is difficult to remove in the post printing steps. Finally, the chamber had to be obtained by a reproducible fabrication technique to facilitate its replacement if necessary.

The chamber (Figure 1(a)) consisted of a spherical body with three inlets and one outlet at 90° from each other. The two side inlets were connected to 5 mL syringes containing the materials, while the upper inlet was connected to the sonicator. The side and upper inlets had a funnel shape to prevent the breakage due to material entrance and probe vibrations, respectively. The outlet was designed to be connected to a needle. The internal volume of the mixing chamber had to be lower than 2 mL to reduce material waste and to be balanced with the volume of the reservoirs. Thus, the chamber internal radius was chosen to obtain its complete filling with 1.2 mL of printing material. The thickness of wall was set to 4 mm to let chamber to absorb ultrasonic waves without breaking (Figure 1(b)). The sonicator used in this work was the VC130 (Sonics&Material INC., USA). The scheme of the connections is shown in Figure 1(d).

A chamber prototype was fabricated by stereolithography (Figure 1(c)). Form2 system and Flexible Resin® from FormLabs® were used.[27,28] The funnels of the inlets were filled with silicone (EcoFlex™) caps able to prevent a leakage of the material from lateral inlets by ensuring a hermetic closure and to elastically deform in response to vibrations of the ultrasonic probe.

The designed mixing chamber was integrated on a customized 3D-bioprinter consisting of two heated piston-driven extruders actuated by stepper motors (Figure 1(d)). To obtain a tunable mixing of the material composition, the chamber was connected to two different reservoirs which eject material at different rates controlled by the revolutions per minutes of the motors. The ratio can be changed during printing phase, thanks to the mixing extruder function configured in the bioprinter firmware (Marlin version 1.1.0-1[29]). The final setup of the 3D-printer is shown in Figure 1(e).

Material preparation

In order to validate the mixing chamber and to optimize the mixing process, gelatin- and nanohydroxyapatite-based composites were prepared. The two reservoirs were

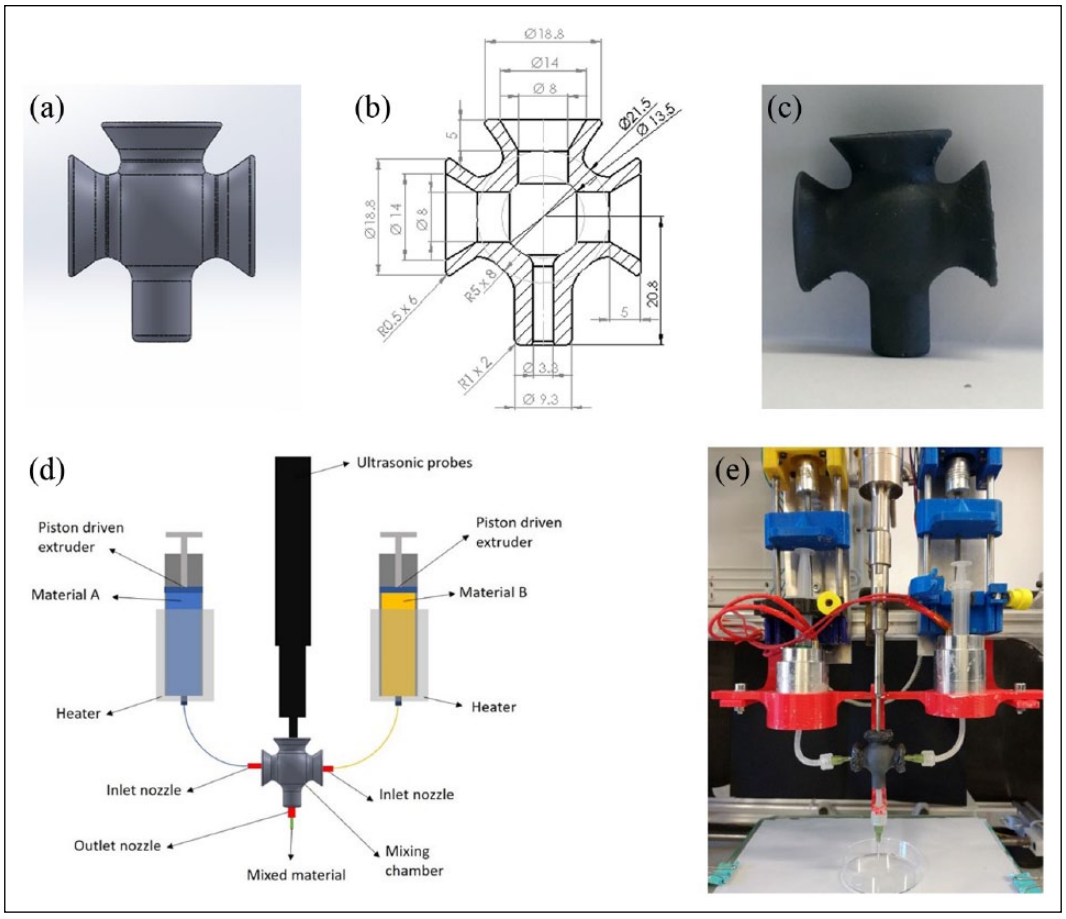

Figure 1. (a) CAD model of the mixing chamber, (b) CAD design of the chamber with main dimensions highlighted: internal structure is visible, (c) mixing chamber 3D-printed by stereolithography, (d) schematic of the connection of the mixing chamber to the sonicator and material reservoirs, and (e) final setup of the 3D-bioprinter with the mixing chamber, ultrasonic probe, and support structure.

filled with two different materials called A and B, respectively (Figure 1(d)).

Material A was obtained by stirring type A gelatin (Sigma-Aldrich®, Italy) at 10% w/v in deionized water at 50°C for 1 h. Subsequently, nanohydroxyapatite (nanoX-IMHAp; Fluidinova, Portugal) 60% w/v (3 g in 5 mL of gelatin solution for each printing test) was added and mixed for 3 min by using a sonicator (equal to the one mounted on the 3D bioprinter) at 20 kHz frequency and 10% amplitude. Finally, genipin (Challenge Bioproduct Co.®, Taiwan) 0.2% w/v was added to the mixture and sonicated for 1 min.

Material B was obtained by adding genipin 0.2% w/v to 10% w/v gelatin solution and sonicating for 1 min (0.01 g in 5 mL of gelatin solution for each printing test).

To prevent nanohydroxyapatite sedimentation and genipin–gelatin reaction during the bioprinting phase, A and B were prepared at each printing.

As proof of concept of the capability of the developed tool to bioprint a 3D-graded structure with clinically relevant dimensions, a ceramic material (Zeolite powder 13X, Alfa-Aesar: Bentonite, Sigma-Aldrich: Colloidal Silica, Sigma-Aldrich with a ratio 2:1:1 w/w) with shape retention properties was used. Two different solutions were prepared, adding a blue dye in one of them.

Identification of the optimal mixing time

Sample preparation. Monolayer lines (40 mm length) were printed after 0, 30, and 60 s of sonication at 50:50 motors percentage ratio. As a control, monolayer lines of only A, only B, and lines obtained with manual mixed material were bioprinted. For each condition and control, three samples were analyzed. In this experiment, no genipin was added. After printing, samples were dried before analysis. During this experiment, the temperature of the mixing chamber was monitored using an external k-type thermocouple.

Micro-computed tomography. To evaluate nanohydroxyapatite distribution inside the printed lines, micro-computed tomography (micro-CT) analysis was performed using a Skyscan11® (Bruker, USA).

Table 1. Main printing parameters used in all printing experiments.

Printing parameter	Value
Printing temperature (°C)	32
Print speed (mm/s)	8
Flow rate %	130
Nozzle size (mm)	1.37
Layer height (mm)	0.4

Micro-CT images were analyzed with ImageJ®, tracing plot profile at a predefined cross section line to evaluate gray-level distribution. For each image, histogram of gray levels was obtained to compare gray-level distribution using MATLAB® (The Mathworks, USA).

Kruskal–Wallis multiple comparison test followed by a Mann–Whitney pairwise comparison test was used to determine whether there was a statistically significant difference ($p = 0.05$) between gray-level distributions. Finally, Mann–Whitney test was used to determine whether there was a significant difference between gray-level distribution of line obtained by manual and chamber mixed material.

Validation of the mixing tool efficiency

Sample preparation. Cylindrical composite samples, obtained with two different methods, were prepared. A first group of samples (10 mm diameter, 6 mm height) was obtained by extruding A and B through the mixing system. Particularly, extruders ratio were tuned (A:B 100:0, 80:20, 50:50, 20:80, 0:100, respectively) to control the volumes of A and B in the chamber, where they were mixed for the optimal time previously identified.

A second group (equal dimensions) was prepared by 3D-bioprinting using a single extruder. In this case, the printed material was prepared by manually sonicating A and B. After printing, samples were left crosslinking for 48 h at room conditions.[26]

Samples with the same nanohydroxyapatite contents were compared through mechanical properties and thermogravimetric analysis (TGA) to evaluate the efficiency of the developed mixing tool.

Other main printing parameters were kept constant, as reported in Table 1. Heaters temperature was set to 32°C to prevent material gelation. The dimension of the printed strands was automatically set equal to the nozzle size. All experiments were performed in triplicate.

Mechanical characterization. Mechanical characterization was carried out performing uniaxial compression tests using a uniaxial testing machine Zwick-Roell Z005 Pro-Line equipped with a 100-N load cell. Before testing, cylindrical samples were fully swollen for 6 h (plateau reached) in deionized water at 37°C.[25] They were compressed until 30% of deformation and strain rate was set to 1% s^{-1} of the initial height. Stress–strain curves were obtained, and elastic modulus was evaluated. Statistically significant differences ($p < 0.05$) between two types of samples were analyzed by a two-tailed *t*-test for unpaired groups.

TGA. Thermal degradation was measured using a TA Instruments Thermobalance model Q5000IR under a nitrogen atmosphere (25 mL/min). The experiments were performed at a 10°C/min heating rate in the 30–800°C temperature range. The amount of sample in each TGA measurement varied between 2 and 4 mg. For each condition, three samples were analyzed. Statistically significant differences ($p < 0.05$) between manual and chamber mixed material were analyzed by a two-tailed *t* test for unpaired groups.

Evaluation of graded structure printability

The capability of getting a graded structure was investigated by printing a monolayer comb. The motor ratio was changed every two teeth to obtain decreasing amount of nanohydroxyapatite, from A:B 100:0, to A:B 0:100. Teeth in the middle were printed with decreasing ratio between A and B. To analyze the amount of nanohydroxyapatite in the teeth, micro-CT images of each tooth were acquired by micro-CT scanner Skyscan11 and analyzed tracing plot profile at a predefined cross-section line. Analysis of variance (ANOVA) multiple comparison was used to determine whether there was a statistically significant difference ($p < 0.05$) between average gray levels for each ratio (three samples analyzed).

Finally, a cylindrical structure with a continuous material gradient was bioprinted as a proof of concept of the capability of the designed mixing tool to bioprint a 3D-graded structure with a clinically relevant size. The Zeolite-based material was used, and the mixing chamber was never totally emptied allowing to obtain a graded change of the ceramic materials contained in the reservoirs.

Results

Identification of optimal mixing time

The optimal mixing time was identified by printing monolayer lines at 0, 30, and 60 s of mixing (Figure 2(a)–(d)) and analyzing micro-CT images of the lines (Figure 2(e)–(h)). Thanks to the presence of calcium atoms, which directly influence the attenuation coefficient, nanohydroxyapatite distribution can be evaluated in the micro-CT image and A can be distinguished from B. As Figure 2 shows, without sonication (0 s), the two solutions were not mixed at all; indeed, clusters of nanohydroxyapatite could be easily distinguished. Clusters became less evident at

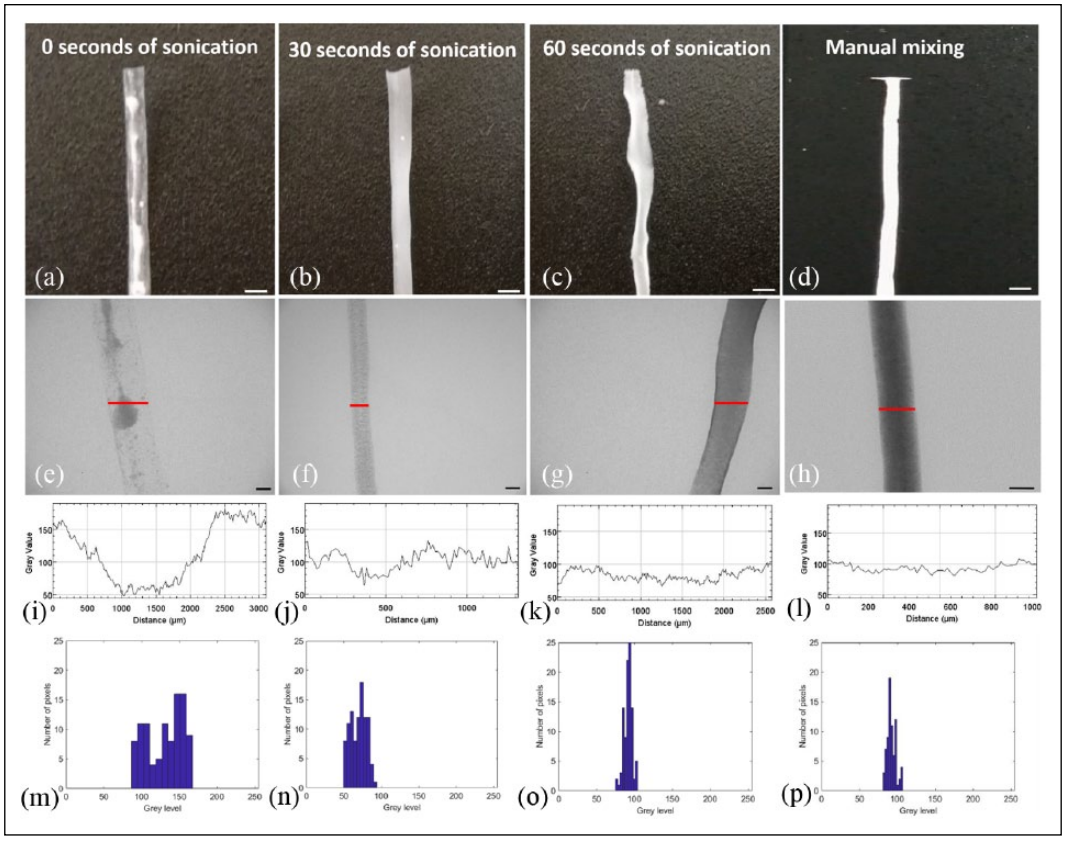

Figure 2. Photos of (a)–(c) monolayer lines at different sonication time and (d) manual mixed line (scale bar = 3 mm). Micro-CT images (e)–(g) of the lines, for each time point and (h) manual mixed line. Red line indicates where plot profiles were traced (scale bar = 1 mm). Nanohydroxyapatite distribution can be evaluated due to its higher attenuation coefficient than gelatin. In (e), dark clusters are nanohydroxyapatite aggregates that are not mixed without sonication. (i)–(l) Plot profile of each line and (m)–(p) gray-level histograms show the narrowing of gray-level distribution of the line with sonication time and therefore an increasingly homogeneous outlet material. Mann–Whitney test highlighted that there are no statistically significant differences between manual and 60 s chamber mixed line.

30 s and are absent after 60 s. The temperature in the mixing chamber was always below 60°C. Plot profiles are presented in Figure 2(i)–(l) and show that gray-level distribution is wider at 0 s and decreases at 30 s, becoming almost constant at 60 s. Gray-level histograms (Figure 2(m)–(p)) confirm the narrowing of the distribution, increasing the sonication time: homogeneity of the outlet material increases with sonication time.

Kruskal–Wallis test and pairwise comparison highlighted a statistically significant difference between all the distribution ($p < 0.001$). In addition, Mann–Whitney test indicates that there is not a statistically significant difference ($p > 0.05$) in the gray-level distribution between chamber (60 s) and manual mixed line.

Validation of the mixing tool efficiency

The elastic modulus of the manual (Figure 3(a)–(c)) and chamber (Figure 3(b)–(d)) mixed cylindrical samples was compared in order to evaluate the functional efficiency of the proposed system. For each concentration and mixing method, three samples were tested. After crosslinking, samples show decreasing dimensions with increasing B content. This behavior is due to a higher gelatin content which turns into a larger water loss. Elastic moduli of different samples are shown in Figure 3(e)–(i). A two-tailed *t* test for unpaired groups was carried out on samples with the same material ratio, but obtained with different mixing methods. There is no difference ($p > 0.05$) between the two types of mixing, proving the efficiency of the developed tool.

The thermogravimetric plots of the composite scaffolds were used to determine the nanohydroxyapatite content in the samples, comparing the residual weight of the samples obtained with different mixing methods (Figure 4). A two-tailed *t* test for unpaired groups was carried out. It showed that there is no statistically significant difference ($p > 0.05$) between the two types of mixing, confirming the efficiency of the developed mixing tool. Red line in the figure indicates the theoretically estimated nanohydroxyapatite amounts inside each sample after drying. Considering, for

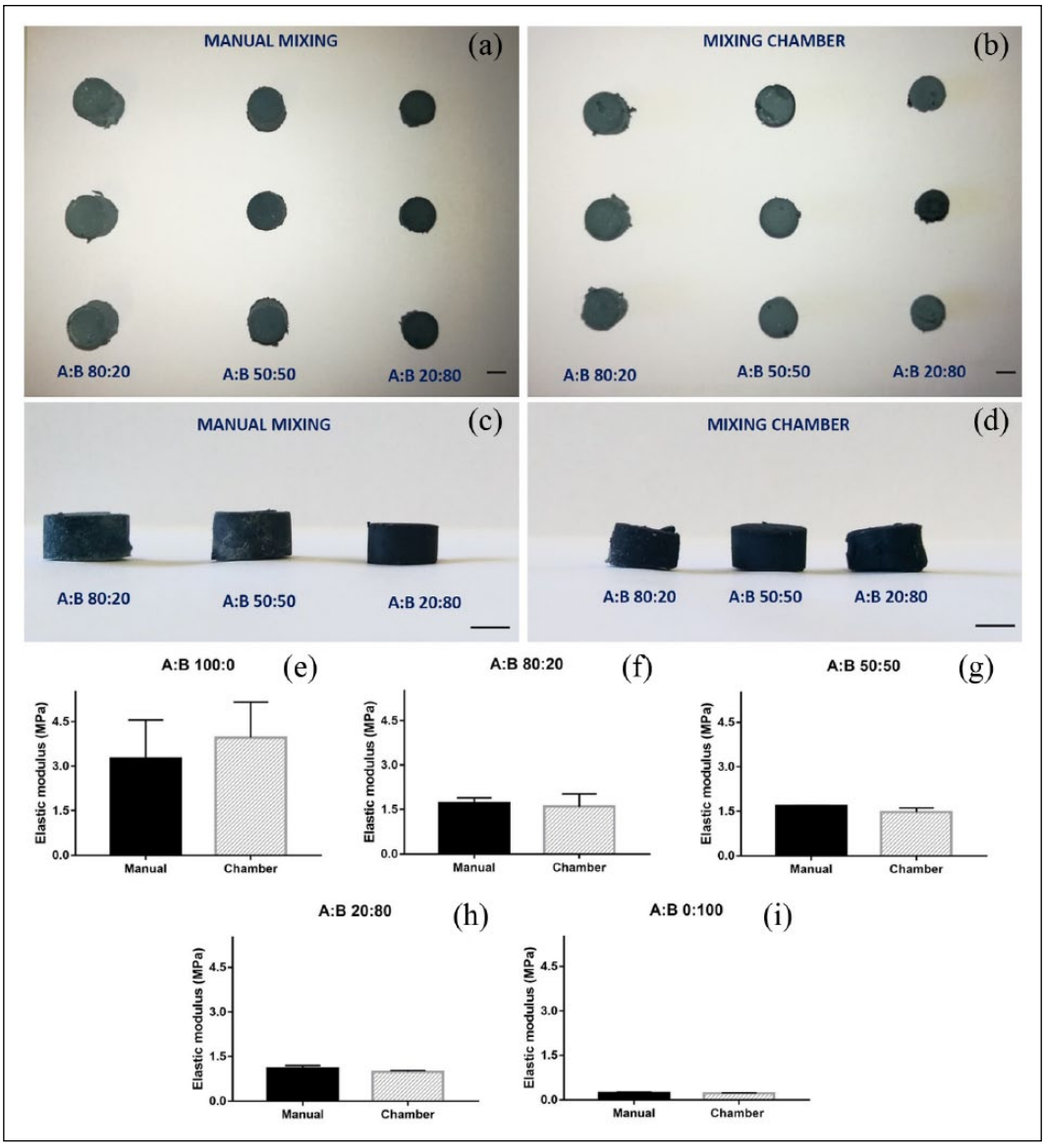

Figure 3. Dried extruded cylindrical samples with A:B 80:20, 50:50, 20:80 percentage ratios obtained by manual mixing ((a) top view and (c) lateral view) and by mixing chamber ((b) top view and (d) lateral view). Scale bar = 3 mm. Comparison between elastic moduli of samples obtained by manual and chamber mixing at different A:B ratios: (e) 100:0, (f) 80:20, (g) 50:50, (h) 20:80, and (i) 0:100. There is no statistically significant difference between the mixing methods in samples with the same hydroxyapatite content.

example, 10 mL of A:B 80:20 material, in the final solution, there are 8 mL of A (containing 0.8 g of gelatin and 4.8 g nanohydroxyapatite, according to material preparation described in the "Material preparation" section) and 2 mL of B (containing 0.2 g gelatin). Consequently, the expected concentration of nanohydroxyapatite in the dried material is $(4.8g / 5.8g) \cong 0.83\% \rightarrow 83\%$.

Evaluation of graded structure printability

To evaluate the feasibility of printing graded structures, a monolayer comb was fabricated (Figure 5(a)). Micro-CT images of each tooth were acquired (Figure 5(b)) and analyzed, tracing the plot profile (Figure 5(c)). Figure 5(d) shows an increase of average gray level with a decrease in the ratio between A and B, proving a decrease in the nanohydroxyapatite content in the line. ANOVA test and pairwise comparison highlighted statistically significant differences between average gray levels ($p < 0.001$), confirming the previous results.

A 3D graded structure with a clinically relevant size was successfully printed (Figure 6). The concentration gradient, due to the presence of the blue dye into one of two mixed materials, is clearly visible.

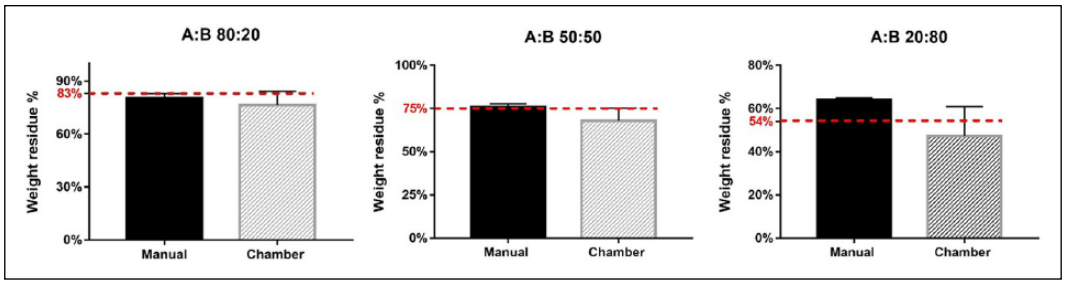

Figure 4. Weight residue obtained from TGA. There are no statistically significant differences between samples obtained with manual or chamber mixing. Red lines represent the theoretical amount of nanohydroxyapatite inside each sample after drying.

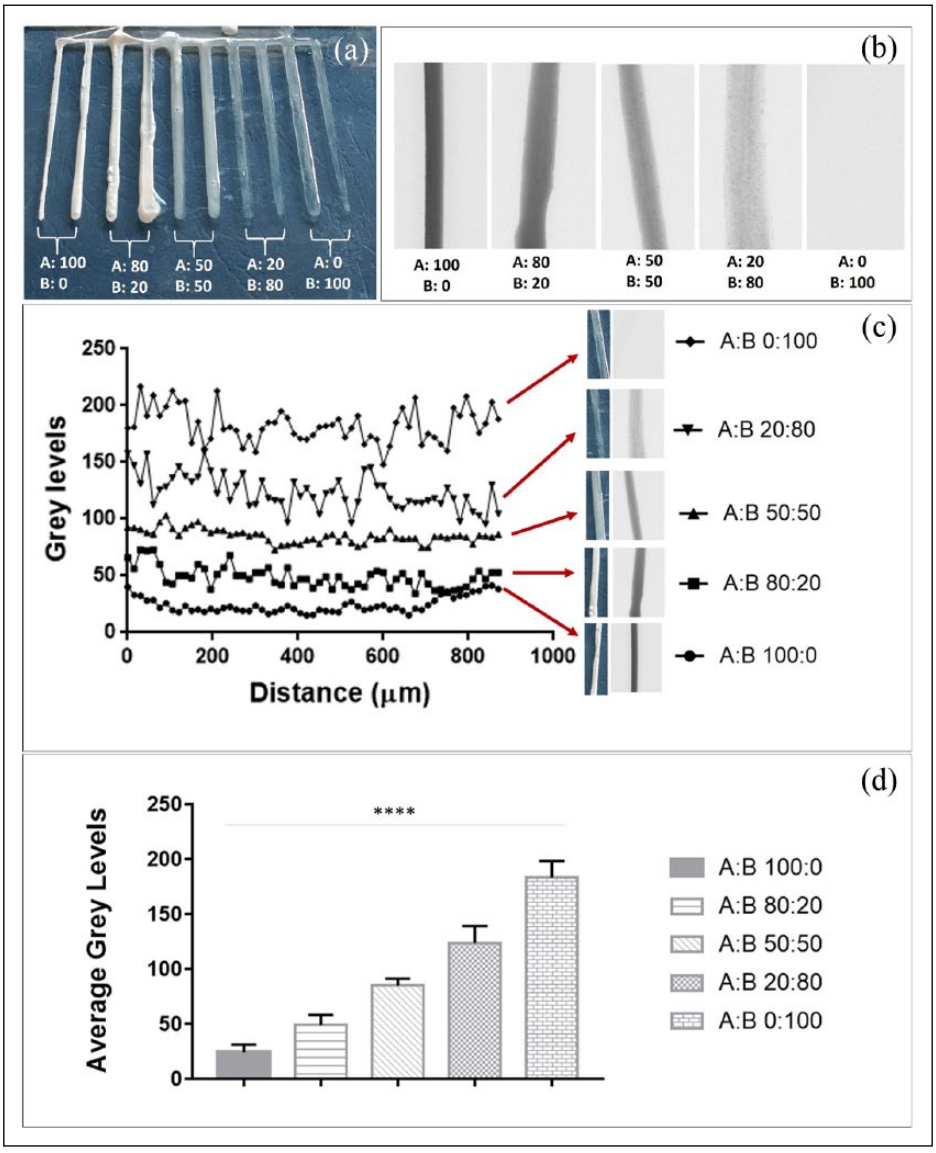

Figure 5. Printing of comb structure: (a) A and B represent ratio between motors. (b) Micro-CT images of comb teeth, showing the decreasing amount of nanohydroxyapatite with the decrease in motor ratio. (c) Plot profile of micro-CT images of each tooth and (d) average gray levels. An ANOVA test and pairwise comparison showed that there is a statistically significant difference (****$p < 0.001$) between the average gray level of each tooth.

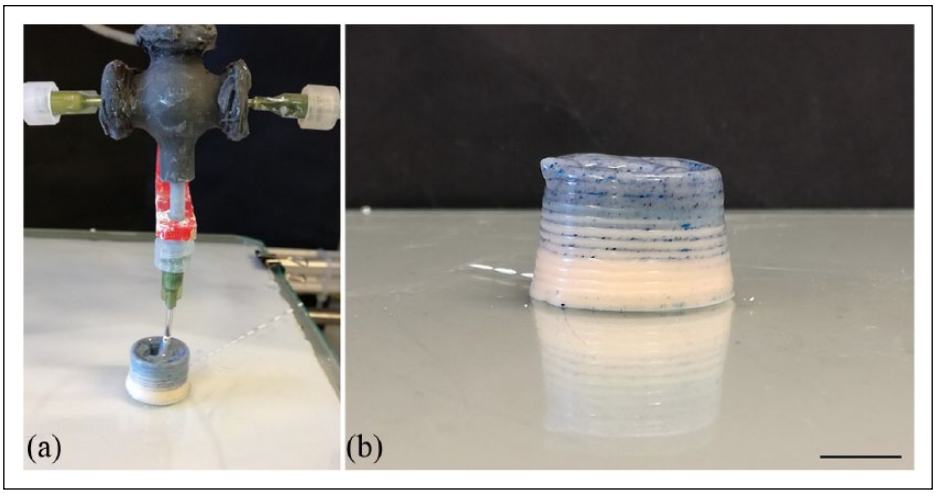

Figure 6. (a) Bioprinting phase of the 3D-graded structure. (b) Final result of the 3D-graded structure: blue dye concentration gradient is clearly visible (scale bar = 1 cm).

Discussion and conclusion

In this work, we presented an innovative mixing tool that could be used for a homogeneous mixing of different materials to be used during biofabrication process of graded scaffold for the regeneration of interface tissues. Different material slurry can be easily printed and mixed with this tool, for example, hydroxyapatite, tricalcium phosphate, and Bioglass®.[1,9,30]

The analysis of micro-CT images allowed to identify the optimal sonication time to obtain a homogeneous mixing of the composite. Results showed that a sonication time of 60 s was sufficient to obtain a homogeneous dispersion of nanohydroxyapatite in gelatin matrix. Limiting the sonication time to a minimum is fundamental to avoid an excessive rise in the chamber temperature, which would cause a decrease in the viscosity of the composite,[31] making it non-printable, due to the poor ability in shape retention after deposition.[32] For our specific test, also crosslinking by genipin is strongly dependent on temperature.[33,34] This process is, in fact, accelerated by temperature increase and may cause the clogging of the needles making it impossible to print. A compressive mechanical characterization and TGA on cylindrical samples proved the good efficiency of mixing with the chamber compared to the manual one, showing comparable elastic moduli and weight residual within each group of samples, respectively.

The new designed system has also proved effective in modulating the quantities of the two extruded materials by controlling the stepper motors revolution ratio, as illustrated by cylindrical graded bioprinted structure. In this specific test, we chose a ceramic material due to its shape retention properties that allowed the printed structure to be self-sustained also for higher heights. Bioprinting a graded structure with a soft material (as nanohydroxyapatite–gelatin solution used for the previous tests) required a support material,[35] so further investigations are needed.

The capability of gradually modulating the amount of different extruded materials is the main advantage of this innovative chamber compared to traditional manual mixing which would not allow to vary the percentages of the two solutions extruded during the printing phase. Thanks to the mixing chamber, it will be possible to bioprint graded scaffolds that will find promising applications in ITE, for example, in bone–cartilage interface.

Declaration of conflicting interests

The author(s) declared no potential conflicts of interest with respect to the research, authorship, and/or publication of this article.

Funding

The author(s) disclosed receipt of the following financial support for the research, authorship, and/or publication of this article: This work was supported by IMAGO project (MX18MO06) funded by MAECI and AMEXIC.

References

1. Seidi A, Ramalingam M, Elloumi-Hannachi I, et al. Gradient biomaterials for soft-to-hard interface tissue engineering. *Acta Biomater* 2011; 7(4): 1441–1451.
2. Criscenti G, Longoni A, Di Luca A, et al. Triphasic scaffolds for the regeneration of the bone–ligament interface. *Biofabrication* 2016; 8(1): 015009.
3. Criscenti G, De Maria C, Longoni A, et al. Soft-molecular imprinted electrospun scaffolds to mimic specific biological tissues. *Biofabrication* 2018; 10(4): 045005.
4. Patel S, Caldwell JM, Doty SB, et al. Integrating soft and hard tissues via interface tissue engineering. *J Orthop Res* 2018; 36(4): 1069–1077.
5. Zhang YS and Xia Y. Multiple facets for extracellular matrix mimicking in regenerative medicine. *Nanomedicine* 2015; 10(5): 689–692.
6. Deluzio TGB, Seifu DG and Mequanint K. 3D scaffolds in tissue engineering and regenerative medicine: beyond

structural templates? *Pharm Bioprocess* 2013; 1(3): 267–281.
7. Chan BP and Leong KW. Scaffolding in tissue engineering: general approaches and tissue-specific considerations. *Eur Spine J* 2008; 17(Suppl. 4): 467–479.
8. Mikos AG, Herring SW, Ochareon P, et al. Engineering complex tissues. *Tissue Eng* 2006; 12(12): 3307–3339.
9. Bracaglia LG, Smith BT, Watson E, et al. 3D printing for the design and fabrication of polymer-based gradient scaffolds. *Acta Biomater* 2017; 56: 3–13.
10. Deng, Y and Jordan, K (eds). *Functional 3D tissue engineering scaffolds: materials, technologies, and applications*. Duxford: Woodhead Publishing, 2017.
11. Groll J, Boland T, Blunk T, et al. Biofabrication: reappraising the definition of an evolving field. *Biofabrication* 2016; 8(1): 013001.
12. Moroni L, Boland T, Burdick JA, et al. Biofabrication: a guide to technology and terminology. *Trends Biotechnol* 2018; 36(4): 384–402.
13. Hutmacher DW. Scaffold design and fabrication technologies for engineering tissues—state of the art and future perspectives. *J Biomater Sci Polym Ed* 2001; 12(1): 107–124.
14. Monzón M, Liu C, Ajami S, et al. Functionally graded additive manufacturing to achieve functionality specifications of osteochondral scaffolds. *Biodes Manuf* 2018; 1(1): 69–75.
15. Woodfield TB, Malda J, de Wijn J, et al. Design of porous scaffolds for cartilage tissue engineering using a three-dimensional fiber-deposition technique. *Biomaterials* 2004; 25(18): 4149–4161.
16. Sobral JM, Caridade SG, Sousa RA, et al. Three-dimensional plotted scaffolds with controlled pore size gradients: effect of scaffold geometry on mechanical performance and cell seeding efficiency. *Acta Biomater* 2011; 7(3): 1009–1018.
17. De Maria C, Vozzi G and Moroni L. Multimaterial, heterogeneous, and multicellular three-dimensional bioprinting. *Mrs Bull* 2017; 42(8): 578–584.
18. Malda J, Visser J, Melchels FP, et al. 25th anniversary article: engineering hydrogels for biofabrication. *Adv Mater* 2013; 25(36): 5011–5028.
19. Liu W, Zhang YS, Heinrich MA, et al. Rapid continuous multimaterial extrusion bioprinting. *Adv Mater* 2017; 29(3): 1604630.
20. Snyder J, Son AR, Hamid Q, et al. Hetero-cellular prototyping by synchronized multi-material bioprinting for rotary cell culture system. *Biofabrication* 2015; 8(1): 015002.
21. Capretto L, et al. Micromixing within microfluidic devices. In: Lin B (ed.) *Microfluidics*. Berlin; Heidelberg: Springer, 2011, pp. 27–68.
22. Chiu Ferreira J, Luo TJ, Geng H, et al. Direct scaffolding of biomimetic hydroxyapatite-gelatin nanocomposites using aminosilane cross-linker for bone regeneration. *J Mater Sci Mater Med* 2012; 23(9): 2115–2126.
23. Azami M, Tavakol S, Samadikuchaksaraei A, et al. A porous hydroxyapatite/gelatin nanocomposite scaffold for bone tissue repair: in vitro and in vivo evaluation. *J Biomater Sci Polym Ed* 2012; 23(18): 2353–2368.
24. Vozzi G, Corallo C, Carta S, et al. Collagen-gelatin-genipin-hydroxyapatite composite scaffolds colonized by human primary osteoblasts are suitable for bone tissue engineering applications: in vitro evidences. *J Biomed Mater Res A* 2014; 102(5): 1415–1421.
25. Jelen C, Mattei G, Montemurro F, et al. Bone scaffolds with homogeneous and discrete gradient mechanical properties. *Mater Sci Eng C: Mater Biol Appl* 2013; 33(1): 28–36.
26. Montemurro F, De Maria C, Orsi G, et al. Genipin diffusion and reaction into a gelatin matrix for tissue engineering applications. *J Biomed Mater Res B: Appl Biomater* 2017; 105(3): 473–480.
27. https://formlabs.com/media/upload/SDS_Resina_Flexible.pdf (accessed December 2018).
28. https://formlabs.com/media/upload/Flexible-DataSheet.pdf (accessed December 2018).
29. http://marlinfw.org/ (accessed December 2018).
30. Gentile P, Mattioli-Belmonte M, Chiono V, et al. Bioactive glass/polymer composite scaffolds mimicking bone tissue. *J Biomed Mater Res A* 2012; 100(10): 2654–2667.
31. Seeton CJ. Viscosity-temperature correlation for liquids. In: STLE/ASME international joint tribology conference, San Antonio, TX, 23–25 October 2006. New York: American Society of Mechanical Engineers.
32. Paxton N, Smolan W, Bock T, et al. Proposal to assess printability of bioinks for extrusion-based bioprinting and evaluation of rheological properties governing bioprintability. *Biofabrication* 2017; 9(4): 044107.
33. Yunoki S, Ohyabu Y and Hatayama H. Temperature-responsive gelation of type I collagen solutions involving fibril formation and genipin crosslinking as a potential injectable hydrogel. *Int J Biomater* 2013; 2013: 620765.
34. Nickerson MT, Patel J, Heyd DV, et al. Kinetic and mechanistic considerations in the gelation of genipin-crosslinked gelatin. *Int J Biol Macromol* 2006; 39(4–5): 298–302.
35. O'Bryan CS, Bhattacharjee T, Niemi S, et al. Three-dimensional printing with sacrificial materials for soft matter manufacturing. *Mrs Bull* 2017; 42(8): 571–577.